

Effects of confinement on carrier dynamics in $\text{In}_{0.47}\text{Ga}_{0.53}\text{As}$ heterostructures

Sarah Bolton,* Gregg Sucha,[†] and Daniel Chemla
Department of Physics, University of California, Berkeley, California 94720

D. L. Sivco and A. Y. Cho
Bell Laboratories, Lucent Technologies, 700 Mountain Avenue, Murray Hill, New Jersey 07974
 (Received 13 April 1998)

To study the effects of confinement by quantum-well potential discontinuities on ultrafast carrier dynamics, we performed pump-broadband probe studies of a series of $\text{In}_{0.47}\text{Ga}_{0.53}\text{As}$ quantum wells excited 30 meV above the band edge. Our measurements show that the rate of carrier thermalization is well width independent; however, the rate of carrier cooling to the band edge is strongly influenced by confinement. This influence has two separate physical origins. First, the dimensionality dependence of the density of states results in a larger proportion of thermalized electrons that can emit LO phonons in three dimensions than in two. Second, modification of the phonon density of states by the ionic mass discontinuity at the well boundaries may reduce the electron-LO-phonon coupling. [S0163-1829(98)07748-0]

I. INTRODUCTION AND EXPERIMENTAL TECHNIQUE

Ultrafast optical measurements have played a major role in understanding the dynamics of semiconductors. Studies of carrier thermalization and cooling are among the most important of these, as they reveal dynamics that are both critical for device development and of fundamental interest for understanding carrier-carrier and carrier-phonon interactions. No such study, however, has examined the effects of material confinement to quasi-two-dimensions on carrier thermalization dynamics. This question is important for device development, as many high-speed devices are based on quantum confined heterostructures. It is also of importance from a more fundamental perspective. It is known that a number of many-body processes that act on the femtosecond time scale, such as screening, Pauli blocking, and the electron phonon interaction, are altered by confinement to two dimensions. However, real structures may exist in a regime intermediate between the absolute two- and three-dimensional limits, and in this regime very little theoretical or experimental work has been done. Furthermore, the theoretically predicted variations in these interactions with dimensionality have not previously been checked experimentally.

In order to explore the influence of dimensionality on these many-body interactions, we have measured the ultrafast optical properties of a series of $\text{In}_{0.47}\text{Ga}_{0.53}\text{As}/\text{In}_{0.47}\text{Al}_{0.53}\text{As}$ heterostructures with varying quantum confinement. This material system is excellent for studies of confinement because $\text{In}_{0.47}\text{Ga}_{0.53}\text{As}$ has a relatively small band gap (800 meV), which leads to large, weakly bound excitons. The exciton Bohr radius in this system is 290 Å, more than twice that in the more commonly studied material GaAs. Studies of $\text{In}_{0.47}\text{Ga}_{0.53}\text{As}$ are also of technological importance, as its bandgap matches the minimum attenuation wavelength of optical fiber. The thickness of the $\text{In}_{0.47}\text{Ga}_{0.53}\text{As}$ quantum well layers in our heterostructures range from 100 Å (one third the Bohr radius) to 6000 Å (20 times the Bohr radius). The valence- and conduction-

band offsets for the $\text{In}_{0.47}\text{Ga}_{0.53}\text{As}/\text{In}_{0.47}\text{Al}_{0.53}\text{As}$ system are 440 and 630 meV, respectively.

There has been substantial previous work on the ultrafast optical properties of semiconductors;¹ however, the vast majority of this work has been on GaAs and larger band-gap materials. Although studies of both narrow quantum wells (QW's)²⁻⁴ and bulk materials⁵ have been performed, previous experiments in which the transition from two to three dimensions is examined have not been carried out. One study of the effect of confinement on spin relaxation dynamics was performed recently;⁶ however, in this case the variation in confinement was achieved by varying the composition of the barriers, which varies the depth of the wells, rather than their width. Changing the depth of the wells alters the penetration of the wave function into the barrier layers, which is not the case when well width is varied.

In this paper we present pump broadband-probe experiments in which $\text{In}_{0.47}\text{Ga}_{0.53}\text{As}$ heterostructures were excited approximately 30 meV above the lowest bound excitonic state. These experiments allowed us to study the effects of confinement on a number of ultrafast processes. Excitation of a semiconductor by a laser first produces coherent oscillations of population between the valence and conduction bands. For excitation above the gap, however, this regime lasts for a time of order the pump duration, and results in the generation of real carrier populations. The evolution of the population is illustrated in Fig. 1. First, the sharply peaked, nonthermal population (a) thermalizes through Coulomb mediated carrier-carrier scattering to a hot Boltzmann distribution (b). This process is complete within the first picosecond, and is discussed in Sec. II. Next, the hot carriers cool to the lattice temperature by the emission of phonons, eventually resulting in a Fermi distribution in equilibrium with the lattice. The majority of carriers have insufficient excess energy to emit LO phonons, and so cool by the much slower acoustic-phonon emission process. Cooling takes several hundred ps and is discussed in Sec. IV. Our measurements also allow us to observe the influence of confinement on a number of transient nonlinearities, addressed in Sec. III.

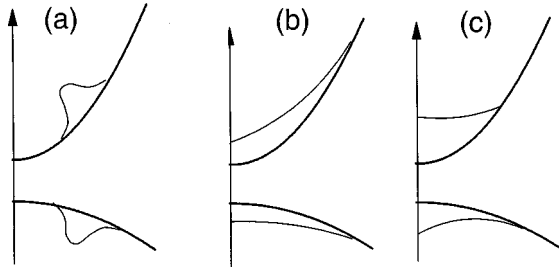


FIG. 1. Schematic of population evolution towards the band edge. (a) 0 fs. Band edge signal is due to screening by the nonthermal population. (b) 300 fs. Band edge signal is due to screening by the hot thermal distribution and Pauli blocking. (c) 20 ps. Band edge signal is due to screening by cooled carriers and Pauli blocking.

Measurements were performed on four $\text{In}_{0.47}\text{Ga}_{0.53}\text{As}/\text{In}_{0.47}\text{Al}_{0.53}\text{As}$ quantum well heterostructures, containing wells of 100, 200, 500, or 6000 Å. The total thickness of $\text{In}_{0.47}\text{Ga}_{0.53}\text{As}$ for all the wells in each sample was 6000 Å. $\text{In}_{0.47}\text{Al}_{0.53}\text{As}$ barriers were 70 Å wide, and the lattice matched InP substrate was mechanically thinned to 50 microns to eliminate signals from two-photon absorption. Linear absorption spectra of the samples are shown in Fig. 2. Pump-probe measurements were performed using continuum generated from a NaCl additive pulse modelocked laser and amplifier system. This system produces 120 fs continuum pulses centered around 1.55 μm . The pump beam was selected from the continuum using appropriate interference filters, while the broadband probe was analyzed using a spectrometer and InGaAs optical multichannel analyzer. All samples were held in a liquid-helium cryostat at 7 K.

The central energy of the pump photons was chosen to be 30 meV above the lowest bound exciton state of each sample. Accounting for the electron and hole effective masses, ($m_{\text{hh}}=0.377m_0$, $m_{\text{lh}}=0.052m_0$, $m_e=0.041m_0$) this excitation produces an initial electron distribution with an excess energy of approximately 26 meV, and a heavy-hole distribution with excess energy approximately 3 meV. $\text{In}_{0.47}\text{Ga}_{0.53}\text{As}$ has two LO-phonon branches, GaAs like, with energy 35 meV, and InAs like, with energy 28 meV. All of the holes and the majority of the electrons thus have in-

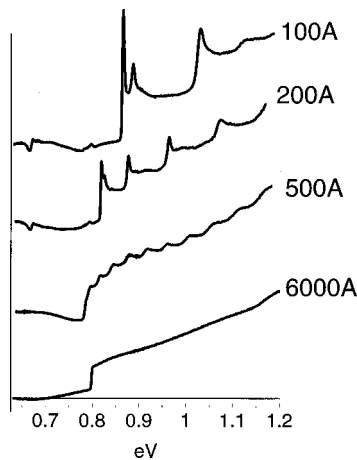


FIG. 2. Linear absorption spectra of four samples, ranging from two to three dimensions.

sufficient energy to emit LO phonons, and will thermalize largely without LO-phonon emission. The absorption spectra for our samples show that for this excitation energy, the density of states for the electrons is very similar, ranging from $\sim 1 \times 10^{16} \text{ meV cm}^{-3}$ in bulk to $\sim 2 \times 10^{16} \text{ meV cm}^{-3}$ in the 100 Å QW's. From the absorption spectra and the depth of the spectral hole we estimate the excitation density for all samples to be $N=5 \times 10^{16} \text{ cm}^{-3}$ distributed over approximately 10 meV. At all times the probe beam waist was less than $\frac{1}{3}$ the pump beam waist, so that the variation in carrier density across the probe was less than 10%.

II. COULOMB INTERACTIONS AND CARRIER THERMALIZATION

Population thermalization by carrier-carrier scattering has been examined both theoretically and experimentally in a number of studies. Because in our experiment electrons are given ten times as much excess energy as holes, our measurements largely reflect electron dynamics. Thermalization requires the exchange of energy among particles, and is thus dominated by interactions between particles of similar mass. Thus, electron-heavy-hole collisions are much less effective in thermalization than are electron-electron scatterings. Although electron-light-hole interactions could also give significant energy rearrangement, the light-hole oscillator strength is only $\frac{1}{3}$ that of the heavy hole, so few light holes are present. Thus we expect thermalization to be dominated by electron-electron scattering.

The scattering rate is governed by two factors: the strength of the (Coulomb) scattering interaction, and the phase space of final states.⁷ The effective strength of the Coulomb interaction is modified by screening; however, accurate models of screening for nonthermal populations are difficult to develop for a number of reasons. First, screening models are strongly dependent on accurate modeling of the k space distribution of the carriers involved.⁸ Simple models generally take either a Fermi or a Boltzmann distribution, leading to the Thomas-Fermi or Debye-Huckel approximations for static screening. For the case of thermalization, however, the population distribution is evolving on a very short time scale, and can not be accurately modeled by any simple functional form. Furthermore, the tractable models for screening generally take a static model, in which the rearrangement of carriers to most effectively screen the potential has no internal dynamics. On the time scales of our experiment, this is clearly not a good approximation. Even these simplified models are only tractable in the absolute two- and three-dimensional regimes, and for wells of finite thickness can only be examined via extensive computational simulations. In addition, these studies rarely include the effects of valence-band complexity, or of many-body effects such as correlations and excitonic effects.

Despite the difficulty in making predictions about the details of carrier thermalization, it has generally been asserted that carrier thermalization should occur faster in quantum wells than in bulk samples due to the reduction in screening in two dimensions. In GaAs quantum wells, pump/broadband probe studies have shown that Coulomb mediated thermalization occurs within 300 fs or less for carrier densities on the order of 10^{10} cm^{-2} .³ Studies have also been performed on

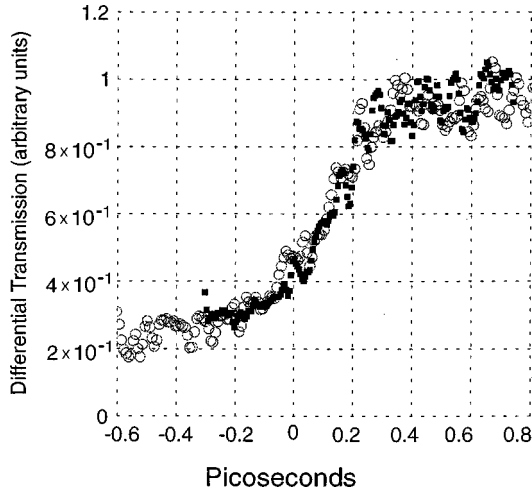


FIG. 3. Differential transmission at band edge near zero time delay. Bulk (gray circles) and 100-Å quantum well (black squares). Signals are averaged over a 20-nm band width.

bulk GaAs,⁵ which found time constants for thermalization approximately twice those found in quantum wells at similar densities, in qualitative agreement with theoretical predictions. Since these experiments were performed with somewhat different techniques and on samples of different quality; however, direct comparison of the results is questionable. Four wave mixing measurements of carrier dephasing in GaAs bulk and quantum wells have also indicated some influence of confinement on screening.^{9,10} However, recent work on spectrally resolved four wave mixing¹¹ has shown that such spectrally integrated measurements can be misleading.

We have measured both detailed dynamics at a single wavelength as well as full spectral information to extract the effects of confinement on carrier thermalization. The signal can be expected to evolve as follows. When the carriers are first injected high in the band, there will be a phase spacing filling signal close to the excitation energy, reflecting the nonthermal electron-hole plasma (hereafter known as the spectral hole). In addition, there will be a signal at the exciton reflecting screening of the exciton by the nonthermal population, which broadens the exciton and reduces its oscillator strength. Once the carriers have thermalized to a hot, Boltzmann distribution the spectral hole will dissipate. The signal at the band edge will simultaneously increase, as it reflects phase space filling of the states that make up the exciton as well as screening of the exciton by the thermalized population. The hot distribution will have a temperature given by the excess energy with which the distribution was initially excited, well in excess of the lattice temperature. Finally, as the carriers cool to the lattice temperature the signal at the band edge will continue to increase, as the occupation of states that overlap the excitonic states increases.

The evolution of the signals at the band edge and spectral hole for $\Delta t < 1$ ps reflect the carrier thermalization dynamics. Figure 3 shows the differential transmission spectrum (DTS) at the band edge for the bulk and 100-Å quantum well samples, over 1.4 ps around $\Delta t = 0$. Contrary to predictions that the thermalization should be substantially faster in two than in three dimensions, the two signals are essentially identical, rising from 10% to 90% of their final value in 400 fs.

Similar measurements taken on samples with 200 and 500 Å well widths give the same results. This indicates, then, that for densities of 10^{16} cm^{-3} the rates of carrier-carrier scattering by the nonthermal population are *not* significantly different in two and three dimensions. Since the densities of both initial and final states are similar among all the samples, the equivalence of carrier-carrier scattering rates implies that, in the range of densities explored, the Coulomb interaction among the nonthermal carriers is equally effective in two and three dimensions. This contradicts the prediction that the Coulomb interaction should be weaker in three dimensions than in two, due to the increased effectiveness of screening. This surprising result is confirmed by the full spectral profiles of the DTS shown in Fig. 4. For all samples, the spectral holes dissipate at the same rate. Using this measure, we confirm our result that the carrier thermalization, and thus efficiency of screening among nonthermal carriers, is not influenced by well width.

III. PAULI BLOCKING AND TRANSIENT BAND-EDGE NONLINEARITIES

The two major influences on the band edge DTS are screening of the Coulomb bound exciton, and Pauli blocking of the excitonic absorption. Pauli blocking, or phase space filling, originates in the fermionic nature of the carriers. The absorption in the presence carriers is $\alpha = \alpha_o(1 - f_e - f_h)$, where f_e and f_h are the electron and hole occupancies, and α_o is the absorption strength in the absence of carriers. The phase space filling nonlinearity, Δ_{psf} , is obtained from the oscillator strengths of the exciton with and without the presence of carriers. In the approximation where the interband matrix elements are taken to be independent of k , the oscillator strength is given by¹²

$$f_n = 4\pi e^2 |r_{cv}|^2 |\phi_n(r=0)|^2 \times \left\{ 1 - \frac{1}{\phi_n(r=0)} \sum_k (f_e + f_h) \phi_n(k) \right\}. \quad (1)$$

Here f_n are the excitonic wave functions and r_{cv} are the interband dipole matrix elements. This leads immediately to the result for the change in oscillator strength due to phase space filling,

$$\frac{\Delta f}{f} = \left\{ \frac{1}{\phi_n(r=0)} \sum_k (f_e + f_h) \phi_n(k) \right\}. \quad (2)$$

We are interested in particular in the effects of phase space filling by a hot carrier distribution. At time delays longer than 500 fs the carriers have already thermalized to a Boltzmann distribution. Carrier cooling through phonon emission does not begin to become significant until at after at least 1 ps of time delay. Thus, the phase space filling contribution to the band edge signal for times between approximately 500 fs and 1 ps is due to a thermalized distribution that has not yet started to lose energy to the lattice. To calculate this contribution, we introduce into Eq. (2) the k space expressions for the excitonic wave functions and the hot carrier distributions in two and three dimensions. For the two-dimensional case, $\phi_{1s}(k) = \sqrt{8\pi\Lambda^2} / [(1 + \Lambda^2 k^2)^{3/2}]$. In three dimensions $\phi_{1s}(k) = \sqrt{64\pi a_o^{3/2}} / [(1 + a_o^2 k^2)^2]$. Here Λ

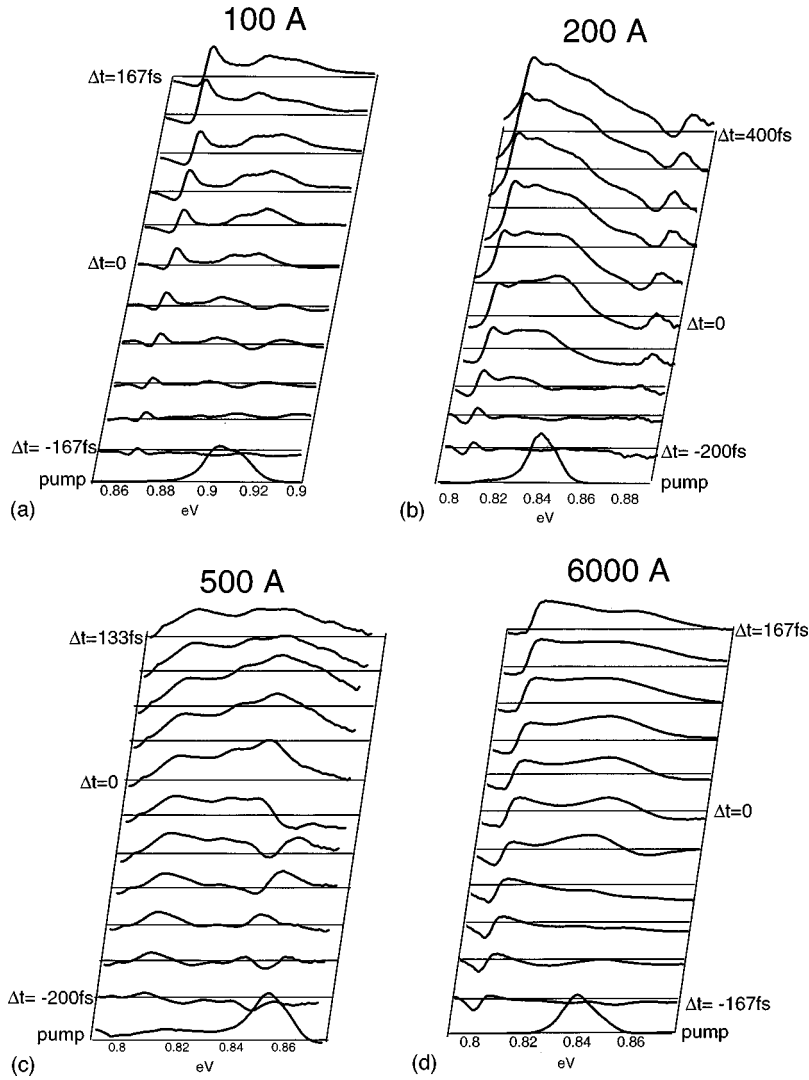


FIG. 4. Time evolution of differential transmission spectra (a) 100-Å well, (b) 200-Å well, (c) 500-Å well, (d) 6000-Å well.

$=a_0/2$. Since the electrons we excite have 30 meV of excess energy, it is legitimate to approximate their distributions with Boltzman distributions. The holes have very little excess energy, so their distributions hardly change with time and can be approximated as Fermi like. We thus obtain for the electron contributions to phase space filling, $S_e = (\pi a_0^2 N_e) 2 \alpha_{e2D} I_{2D}$ in two dimensions, and $S_e = (8 \pi^{1/2} a_0^3 N_e) \alpha_{e3D}^{3/2} I_{3D}$ in three dimensions. Here $\alpha_{e2D} = (m/m_e)(4E_o/kT)$ and $\alpha_{e3D} = (m/m_e)(E_o/kT)$. I_{2D} and I_{3D} are integrals over error functions (see Appendix) that can be evaluated explicitly for any given carrier density (N_e) and excess energy (E_o). For 10^{17} cm^{-3} carriers with an excess energy of 30 meV, we predict that phase space filling will be approximately twice as effective in two as in three dimensions.

For early time delays, when the carriers are in a nonthermal distribution, the signal at the band edge is due entirely to Coulomb interactions, i.e., screening and collisional broadening. Once the carriers have thermalized, phase space filling by the hot population contributes to the signal as well as screening. Thus, by comparing differential absorption spectra around zero time delay with those at 500 fs time delay, we obtain an estimate of the relative importance of screening

and phase space filling in two and three dimensions. In Sec. II we showed that screening does not appear to be strongly affected by confinement for our carrier densities. Thus, a comparison of early to late band edge signals for different well widths gives a measure of the effect of confinement on the strength of phase space filling. Figure 5 shows DTS of the 100 Å quantum well and bulk samples taken at zero time delay and at $\Delta t = 500$ fs. A comparison of the band edge DTS shows that phase space filling (PSF) is approximately

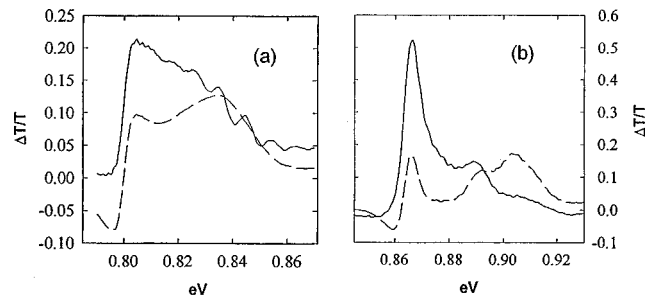


FIG. 5. Differential transmission spectra for zero time delay (dotted) and $\Delta t = 500$ fs (solid). (a) 6000-Å sample, (b) 100-Å sample.

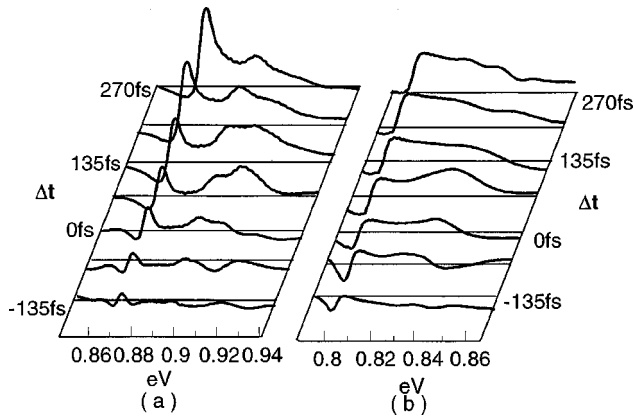


FIG. 6. Differential transmission spectra for (a) 100-Å sample and (b) 6000-Å sample.

twice as effective in the quantum well as in the bulk. This is in good agreement with our calculation. We have measured this ratio in intermediate dimensionality samples, and obtain a linear extrapolation from the two-dimensional to the three-dimensional limit.

Several other nonlinearities occur near the band edge for delays close to $\Delta t = 0$. In all samples, the band edge signal builds up from a small signal that is present well before $\Delta t = 0$. The majority of this signal is due to the coherent contribution to the pump probe response. For above resonance excitation, this coherent contribution is known to produce a DTS that is negative below the resonance and positive at and above the resonance. This signal rises with a time constant T_2 for $\Delta t < 0$, and persists as long as the pump and probe pulses overlap for $\Delta t > 0$.¹³ The DTS for the bulk sample are consistent with such a coherent contribution, as shown in Fig. 6. In the 100- and 150-Å quantum well samples, however, a negative signal below the exciton persists for at least 400 fs, well beyond the overlap of the pump and probe pulses. In these samples the excitons are very strongly bound, yielding large oscillator strengths. These excitons undergo collisional broadening due to the electron hole plasma excited by the pump. We believe it is this incoherent collisional broadening which causes the longer lived negative signal. Although the weaker excitons in the wider samples are almost certainly broadened as well, due to the fact that the excitonic resonances are less well defined collisional broadening is less evident. The change in exciton linewidth can be related to the excitation induced dephasing effects discussed in recent four wave mixing experiments.^{14,15} However, in our case the time scale of the measurement is substantially greater than the dephasing time of the carriers (due to the relatively long pulses and the very short dephasing time induced by the high free-carrier density.) Thus the change in exciton linewidth is more appropriately described as incoherent collisional broadening.

IV. ELECTRON-PHONON INTERACTIONS

Interactions between carriers and lattice vibrations allow hot carriers to cool to the lattice temperature, which is, on a long time scale, in equilibrium with the surroundings. Studies of these interactions have become quite active in the past decade, as carrier cooling dynamics are critical to the recov-

ery times of many devices. These studies have in large part been restricted to the electron phonon interaction, because the hole phonon interaction is greatly complicated by the complexity of the valence-band structure. In our experiments, it is legitimate to concentrate on cooling of the electrons, as they have the large majority of excess energy. For our experimental regime the effects of high carrier densities on the electron phonon interaction can not be neglected. In this case polar interactions are screened, and the screening must be treated appropriately. A second effect of high carrier densities arises because the rate for hot electrons to emit a LO phonon may be much higher than the rate for LO phonons to decay into acoustic phonons. Since only acoustic phonons can drain energy from the sample and equilibrate it with its surroundings a large population of nonequilibrium LO phonons may develop. These hot phonons decrease the rate of carrier cooling by increasing the likelihood that a carrier will reabsorb a phonon. The effects of hot phonons have been measured in a number of studies in GaAs.^{14,15}

The addition of confinement to this picture introduces a number of new issues. Most obviously, the electronic wave functions must be modified to take account of the confinement. Boundary conditions for doing this are well understood.¹⁶ A more complicated problem is posed by the effect of confinement on the phonon modes. For long-wavelength acoustic modes, the mode frequencies in the well and barrier generally have substantial overlap. In this case, the multiple quantum well structure acts as a superlattice, which leads to zone folding. In many cases, however, this does not introduce a strong perturbation to the strength of the interactions and the acoustic phonons can be treated as bulk modes. For optical phonons, however, the situation is very different. The frequencies of optical modes in the wells and barriers may be very different, making it impossible for phonons to propagate. In this case the phonon modes must be treated as confined. The development of appropriate boundary conditions for these modes remains controversial. In addition to confined versions of ordinary optical modes, there exist also new interface modes whose importance in electron phonon scattering is also the subject of intensive study. The presence of a transition with decreasing well width from propagating to confined phonon modes in GaAs/Ga_{1-x}Al_xAs has been shown in Raman scattering experiments.¹⁷

In the simplest model of confined phonon modes, phonons are taken to have zero amplitude at the barriers, leading to quantization of the wave vectors. Such confined modes will have a weaker polar optical interaction with electrons than do bulk modes, as this interaction goes as $1/q^2$, and for confined modes there exists a minimum q . In addition to these effects other, more subtle effects are produced by confinement. These include a change in the strength of screening of the polar interaction as well as alterations of the overlap of the electron and phonon wave functions. It should be noted that the majority of both experimental and theoretical work on the effects of confinement on the electron phonon interaction have treated electron populations that are very high above the band edge, on the order of 200–400 meV, in lattices that are at room temperature. In this case, the LO phonons are by far the most important as the electrons have a large energy, and there is an equilibrium phonon population that can result in absorption as well as emission

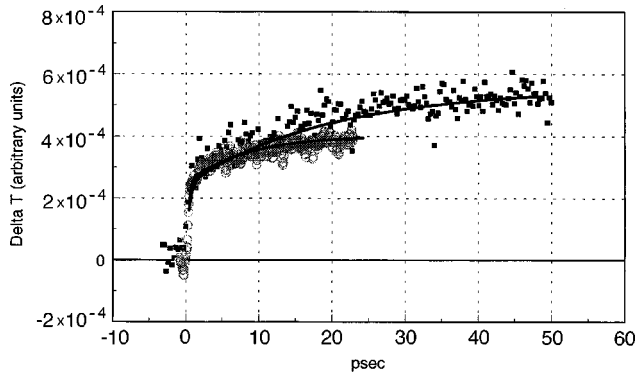


FIG. 7. Band edge differential transmission of bulk (gray circles) and 100-Å quantum well (black squares) samples. Solid lines are double exponential fits to the data, yielding initial rise times of <1 ps for both samples. The long time constant is 20 ps for the quantum well and 7 ps for the bulk.

of phonons. Furthermore, intersubband processes as well as intervalley scatterings are important in this case. In our experiment, the electrons are excited with about 26 meV of excess energy. The lowest LO-phonon mode in $\text{In}_{0.47}\text{Ga}_{0.53}\text{As}$ is at 28 meV, however this InAs-like mode interacts far more weakly with electrons does the GaAs-like mode at 35 meV.¹⁸ Thus, immediately after excitation, less than 5% of the electrons, (and none of the holes) have sufficient energy to emit LO phonons. The LO-phonon modes in $\text{In}_{0.47}\text{Al}_{0.53}\text{As}$ are 10 meV higher at zone center than those in $\text{In}_{0.47}\text{Ga}_{0.53}\text{As}$, and thus we expect confinement of these modes in the narrowest wells.¹⁹

In order to study the influence of confinement on electron

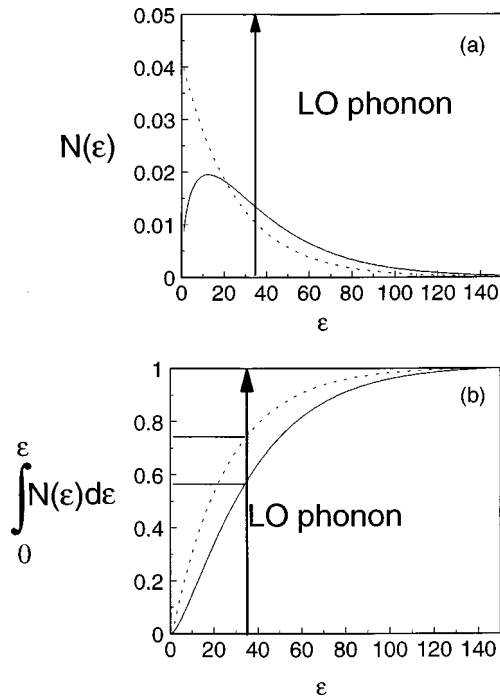


FIG. 8. (a) Thermalized carrier distribution, $N(\epsilon)$, for $kT = 25$ meV. Three dimensions (solid) and two dimensions (dotted). (b) Integrated fraction of carriers with energies less than ϵ , for three dimensions (solid) and two dimensions (dotted). Lowest LO-phonon energy is marked with an arrow.

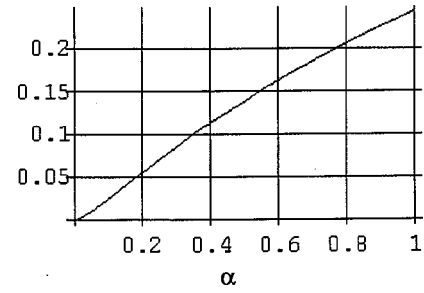


FIG. 9. Three-dimensional integral I_{3D} .

phonon interactions in our samples, we measured the rate of arrival of carriers at the band edge over long times, up to 50 ps. Since carrier thermalization is complete within a few hundred fs, the gradually increasing signal at the band edge reflects the cooling of the electron distribution, which results in a slowly increasing band edge population. Data for the 100-Å quantum well and the 6000 Å bulk sample are shown in Fig. 7. Note that the band edge signal in the bulk saturates considerably faster than does that in the quantum well, indicating that in the bulk sample, the carriers complete their cooling towards a Fermi-Dirac distribution more quickly. Fitting these signals with a simple exponential model, which assumes one phonon scatterings, we find a 7-ps time constant for the bulk, compared to a 21-ps time constant for the quantum well.

One might interpret this difference as a reduction in electron-acoustic phonon scattering due to confinement. However this interpretation is problematic because the time constants are far too short. Typical electron-acoustic phonon scattering times for III-V materials are on the order of 100–300 ps.²⁰ Our scattering times are far more consistent with those obtained both theoretically and experimentally for GaAs with sufficiently high carrier densities to cause hot phonon effects. (~ 7 ps).²⁰ The densities we excite, on the order of 10^{11} – 10^{12} cm^{-2} are in this regime.

We interpret the difference in our measured cooling times by considering the Boltzmann distributions the electrons take up once they have thermalized. The electronic distributions in two and three dimensions are given by the product of the Boltzmann distribution and the density of states. In this case the Boltzmann distributions are the same; however, the densities of states near the band edge are very different (rising as energy $1/2$ in three dimensions, independent of energy in 2). Figure 8(a) shows the energy distributions of our thermalized, hot electron populations as calculated from their excess energy. In Fig. 8(b), the populations have been integrated to show the total percentage of carriers below a given energy. In both figures the strongest LO phonon, at 35 meV, is

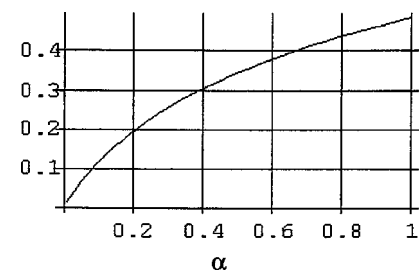


FIG. 10. Two-dimensional integral I_{2D} .

marked. From this figure we see that in the *thermalized* distributions, in contrast to the initial *nonthermal* distribution, a large fraction of the carriers have sufficient energy to cool by emission of LO phonons. This fraction, however, is confinement dependent, being considerably larger in three dimensions (43%) than in two (26%). This difference of carrier distribution accounts for approximately a factor of two difference in bulk and quantum well cooling rates. Our data shows a somewhat larger difference. The additional slowing of electron cooling in the quantum well sample may reflect a reduction of the electron-LO-phonon coupling constant due to confinement. It should be noted that once the electron population has cooled to an average temperature of 20 meV, virtually no carriers remain high enough in energy to emit LO phonons. At this point, acoustic-phonon emission will dominate, and the carrier cooling rate will be vastly reduced. The remaining cooling is expected to take place on the time scale of several hundred picoseconds, which is not experimentally accessible with our present apparatus.

V. CONCLUSIONS

Our studies of carriers excited well above the band edge in $\text{In}_{0.47}\text{Ga}_{0.53}\text{As}$ heterostructures have several results. We find that carrier thermalization to a hot, Boltzmann distribution occurs within 400 fs of excitation, and is independent of well width. This indicates that the Coulomb interaction among carriers is not strongly modified by confinement at our densities. Pauli blocking of the exciton by this hot distribution, however, is influenced by confinement, being approximately twice as effective in two dimensions as in three,

and extrapolating linearly between the two- and three-dimensional limits. The relative strength of this nonlinearity in two and three dimensions agrees well with our calculations.

Dynamics on longer time scales are also affected by confinement, due to a modification of the efficiency of electronic cooling by phonon emission. Confinement influences this process in two ways. First, the dimensionality dependence of the density of states results in a higher proportion of the thermalized electron distribution that can emit LO phonons in three dimensions than in two. Second, confinement of the phonons by the ionic mass difference between barriers and wells may result in a modified phonon density of states, reducing the electron-LO-phonon coupling.

ACKNOWLEDGMENTS

This work was supported by the Director, Office of Energy Research, Office of Basic Energy Sciences, Division of Material Sciences of the U.S. Department of Energy, under Contract No. DE-AC03-76SF00098.

APPENDIX: MATHEMATICAL DETAILS OF PHASE SPACE FILLING CALCULATION

The integral I_{3D} that appears in Sec. III is given by $I_{3D} = \int_0^\infty \{(\alpha^{3/2} e^{-\alpha x} \sqrt{x}) / [(1+x)^2]\} dx$, evaluated in Fig. 9. The integral I_{2D} is given by $I_{2D} = \int_0^\infty \{(\alpha e^{-\alpha x}) / [(1+x)^{3/2}]\} dx$, and is evaluated in Fig. 10. The α are defined for two and three dimensions in Sec. III.

*Permanent address: Department of Physics, Williams College, Williamstown, MA 01267.

†Permanent address: IMRA America, 1044 Woodridge Avenue, Ann Arbor, MI 48105.

¹See, for a review, *Hot Carriers in Semiconductor Nanostructures*, edited by Jagdeep Shah (Academic, San Diego, 1992).

²W. H. Knox, D. S. Chemla, G. Livescu, J. E. Cunningham, and J. E. Henry, Phys. Rev. Lett. **61**, 1290 (1988).

³W. H. Knox, C. Hirlimann, D. A. B. Miller, J. Shah, D. S. Chemla, and C. V. Shank, Phys. Rev. Lett. **56**, 1191 (1986).

⁴J. B. Stark, W. H. Knox, and D. S. Chemla, Phys. Rev. Lett. **68**, 3080 (1992).

⁵J. L. Oudar, D. Hulin, A. Migus, A. Antonetti, and F. Alexandre, Phys. Rev. Lett. **55**, 2074 (1985). See, for example, A. Y. Cho, J. Vac. Sci. Technol. **16**, 275 (1979).

⁶I. Brener, W. H. Knox, K. W. Goosen, and J. E. Cunningham, Phys. Rev. Lett. **70**, 319 (1993).

⁷R. D. Mattuck, *A Guide to Feynman Diagrams in the Many Body Problem* (Dover, Toronto, 1992).

⁸R. Zimmerman, Phys. Status Solidi **140**, 371 (1988).

⁹J.-Y. Bigot *et al.*, Phys. Rev. Lett. **67**, 636 (1991).

¹⁰P. Becker *et al.*, Phys. Rev. Lett. **61**, 1647 (1988).

¹¹J.-Y. Bigot, M. A. Mycek, S. Weiss, R. G. Ulbrich, and D. S. Chemla, Phys. Rev. Lett. **70**, 3307 (1993).

¹²S. Schmitt-Rink, D. S. Chemla, and D. A. B. Miller, Phys. Rev. B **32**, 6601 (1985).

¹³C. Brito-Cruz, J. P. Gordon, P. C. Becker, R. L. Fork, and C. V. Shank, IEEE J. Quantum Electron. **24**, 261 (1988).

¹⁴C. L. Collins and P. Y. Yu, Phys. Rev. B **30**, 4501 (1984); D. Kim and P. Y. Yu, Phys. Rev. B **43**, 4158 (1991).

¹⁵K. Kash, J. Shah, D. Block, A. C. Gossard, and W. Wiegmann, Physica B **134**, 189 (1985).

¹⁶G. Bastard, *Wave Mechanics Applied to Semiconductor Heterostructures* (Halstead, New York, 1988), pp. 1–12.

¹⁷D. S. Kim, A. Bouchalkha, J. M. Jacob, J. F. Zhou, J. J. Song, and J. F. Klem, Phys. Rev. Lett. **68**, 1002 (1992).

¹⁸A. M. DePaula and G. Weber, J. Appl. Phys. **77**, 6306 (1995).

¹⁹P. Y. Yu (private communication).

²⁰S. Das Sarma, in *Hot Carriers in Semiconductor Nanostructures*, edited by Jagdeep Shah (Academic, San Diego, 1992), p. 60.